Published for SISSA by Springer

Received: March 4, 2022
Accepted: June 6, 2022
Published: July 11, 2022

Gluon fusion production at NLO: merging the transverse momentum and the high-energy expansions

Luigi Bellafronte,[a] **Giuseppe Degrassi,**[b] **Pier Paolo Giardino,**[a] **Ramona Gröber**[c] **and Marco Vitti**[b]

[a] *Instituto Galego de Física de Altas Enerxías, Universidade de Santiago de Compostela, 15782 Santiago de Compostela, Galicia, Spain*

[b] *Dipartimento di Matematica e Fisica, Università di Roma Tre and INFN, sezione di Roma Tre, I-00146 Rome, Italy*

[c] *Dipartimento di Fisica e Astronomia 'G. Galilei', Università di Padova and INFN, sezione di Padova, I-35131 Padova, Italy*

E-mail: lui.bellafronte@usc.es, giuseppe.degrassi@uniroma3.it, pierpaolo.giardino@usc.es, ramona.groeber@pd.infn.it, marco.vitti@uniroma3.it

Abstract: The virtual corrections to $gg \to HH$ and $gg \to ZH$ are analytically evaluated combining an expansion in the small transverse momentum of the final particles with an expansion valid at high energies. The two expansion methods describe complementary regions of the phase space and we merge their results, extending the range of validity of both expansions using Padé approximants. We show that this approach can reproduce the available numerical results retaining the exact top quark mass dependence with an accuracy below the 1% level. Our results allow a fast and flexible evaluation of the virtual corrections of the considered processes. Furthermore, they are available in different renormalisation schemes of the top quark mass.

Keywords: Higgs Production, Higher-Order Perturbative Calculations

ArXiv ePrint: 2202.12157

Open Access, © The Authors.
Article funded by SCOAP[3].

https://doi.org/10.1007/JHEP07(2022)069

JHEP07(2022)069

Contents

JHEP07(2022)069

1 Introduction

At the Large Hadron Collider (LHC) gluon fusion is the most relevant production mechanism for Higgs physics in single-Higgs production, $gg \to H$, and pair production, $gg \to HH$, and plays an important role in the production of a Higgs boson in association with a Z boson, $gg \to ZH$. Precise predictions for such processes are necessary in order to measure the properties of the Higgs boson accurately. Since the Higgs boson is a colorless particle, these processes are all loop-induced and mediated by a heavy particle, mainly the top quark. As known since more than twenty years, QCD corrections to the Born result are very large and the perturbative expansion converges slowly (see for example [1, 2]). This implies that the knowledge of the higher-order QCD corrections is very important. However, the evaluation of these corrections is extremely challenging already at next-to-leading order (NLO), since it requires the computation of two-loop diagrams.

In this paper we are going to consider the virtual corrections to Higgs production via gluon fusion at the NLO level. In general, the degree of difficulty in the evaluation of loop diagrams grows with the number of energy scales present in the diagram. In the case of single-Higgs production the relevant diagrams feature a triangular topology and, consequently, depend upon only two scales, namely the Higgs mass, m_H, and the top mass,[1] m_t. In this case, the functional dependence of the result upon the top mass can be expressed in terms of one single variable, m_H^2/m_t^2. Due to this "simplified" one-scale situation, exact analytic results for the NLO corrections are available since many years [3–6].

In the case of processes with two particles in the final state the situation is more complicated. Indeed these processes receive contributions not only from triangle diagrams, which can be calculated adapting the exact analytic results obtained for single-Higgs production, but also from box-topology diagrams. In pair production, $gg \to HH$, the box diagrams depend upon four scales, namely $\hat{s}$, $\hat{t}$, m_t, m_H, where $\hat{s}$, $\hat{t}$, and $\hat{u}$ are the Mandelstam variables which satisfy the condition

$$\hat{s} + \hat{t} + \hat{u} = 2\, m_H^2 \ . \tag{1.1}$$

[1] All the quarks but the top are assumed to be massless.

Concerning associated production, $gg \to ZH$, a fifth energy scale is present, i.e. the mass of the Z vector boson, m_Z.

Exact analytic results for two-loop box diagrams with several energy scales cannot be derived with the present computational technology. Instead, usually two different strategies are followed in order to evaluate the two-loop box contribution in Higgs production via gluon fusion. a) A fully numerical exact evaluation [7–11]. b) An approximate analytic evaluation that takes advantage of hierarchies among the various energy scales present in the diagrams, in order to reduce the number of scales in the problem. Thus, its validity is restricted to specific regions of the phase space. The method used is based on the expansion of the diagrams in terms of ratios of small energy scales vs. large energy scales, in order to obtain a result that retains an exact dependence upon the large energy scales. Concerning the small ones, in order to simplify further the evaluation, expansions in term of ratios between small energy scales is often used.

The former strategy, although accurate, is very demanding from a computational point of view, requiring a high degree of optimization in order to obtain a result in a "reasonable", although usually quite long, computer time. Furthermore, this approach is not very flexible with respect to the modification of the input parameters.

Strategy b) provides accurate results valid in specific regions of the phase space without requiring heavy computational work, i.e. in a short computer time. Examples of this approach of evaluating the two-loop box contribution are:

i) The infinite-top-mass limit [12, 13] refined by the inclusion of powers in the large top-mass expansion (LME) [14–17]. Here, m_t is assumed to be the large energy scale while $\hat{s}$, $\hat{t}$, m_H, and in associated production also m_Z, are considered to be the small ones. Thus, the validity of this approach is restricted to phase-space regions where $\hat{s}/(4m_t^2) \leq 1$. The advantage of this approximation are the rather simple results, which can be expressed in terms of rational functions and logarithms of the kind $\log(m_t^2/\hat{s})$.

ii) The evaluation via an expansion in the transverse momentum, p_T, of the final-state particles [18, 19]. Here, $\hat{s}$ and m_t are assumed to be the large energy scale while m_H, m_Z and p_T, that can be traded for $\hat{t}$, are considered to be the small ones. The validity of this approach is restricted to phase-space regions where $|\hat{t}|/(4m_t^2) \lesssim 1$. The analytical complexity of this approach is higher than in i), as generalised polylogarithms and two elliptic integrals occur in the final results. The evaluation of the latter can be easily performed using the results of ref. [20].

iii) The evaluation via a high-energy (HE) expansion [21–23]. Here $\hat{s}$, $\hat{t}$ are assumed to be the large energy scale while m_t, m_H and m_Z, with $m_t \gg m_H$, m_Z, are considered to be the small ones. The validity of this approach is restricted to phase-space regions where $|\hat{t}|/(4m_t^2) \gtrsim 1$. The HE expansion leads to analytic results that can be expressed in terms of harmonic polylogarithms.

iv) The evaluation via an expansion in terms of small external masses [24–26]. Here $\hat{s}, \hat{t}, m_t$ are assumed to be the large energy scale while m_H and m_Z are considered to be

JHEP07(2022)069

the small ones. This approach basically covers the entire phase space of the considered processes. However, since the reduction of scales in this approach is minimal, one ends up with the evaluation of Master Integrals (MIs) that are much more complicated than those appearing in the i)–iii) cases. As a consequence the evaluation of the box contribution in any point of the phase space requires a longer computer time than in the approaches i)–iii).

As an alternative approach, refs. [27, 28] proposed to reconstruct the full result from its LME version, supplemented by the non-analytic part of the diagrams near the top threshold, via a conformal mapping and Padé approximants.

In this paper we propose an alternative way to derive the full top-mass dependence in Higgs production via gluon fusion, based on the merging of the p_T expansion in ii) with the HE expansion in iii) that individually are valid in complementary regions of the phase space. Since the numerical evaluations of the two expansions are quite fast from a computational point of view, our proposal allows a fast evaluation of the virtual corrections to Higgs production via gluon fusion that is accurate in the entire phase space.

The key point of our analysis is to extend the fixed-order results both in the p_T expansion [18, 19] and in the HE expansion [22, 23] up to or beyond their border of validity, i.e. $\hat{t} \simeq 4m_t^2$, in order to merge the two analytic approximations. This is done by constructing a [1/1] Padé approximant for the p_T-result and a [6/6] Padé approximant for the HE-result. We point out that the extension of the HE expansion via Padé approximants has been already considered in refs. [22, 23].

The paper is organized as follows. In section 2 we introduce the different expansions as well as the method for combining them. In section 3 we validate the method at LO both at the level of form factors and at the level of the partonic cross section, with a focus on the $gg \to HH$ process. In section 4 we present the merging of the two expansions at NLO. In order to show the flexibility of our approach with respect to the modification of the input parameters, in the same section we present the result for the two-loop virtual contribution in $gg \to HH$ and $gg \to ZH$ for two different choices of the top quark mass, namely the on-shell and the $\overline{\text{MS}}$ mass. Finally, we conclude in section 5.

2 Method

We start by considering the process $g(p_1)\, g(p_2) \to 3(-p_3)\, 4(-p_4)$, where 3 and 4 are two neutral[2] particles with masses m_3 and m_4, respectively. Taking all momenta to be incoming, the partonic Mandelstam variables are

$$\hat{s} = (p_1 + p_2)^2, \qquad \hat{t} = (p_1 + p_3)^2, \qquad \hat{u} = (p_2 + p_3)^2, \tag{2.1}$$

and the transverse momentum p_T of the final-state particles can be written as

$$p_T^2 = \frac{\hat{t}\hat{u} - m_3^2 m_4^2}{\hat{s}}. \tag{2.2}$$

[2]Dealing with neutral particles in the final state implies the absence of mixed top-bottom diagrams, as they would appear e.g. in $gg \to W^+W^-$ production, for which the proposed method cannot be straightforwardly applied.

JHEP07(2022)069

As suggested in refs. [18, 19], if the amplitude of the process is written in terms of (anti)symmetric form factors with respect to the exchange $\hat{t} \leftrightarrow \hat{u}$, then it is sufficient to discuss only the forward contribution to the cross section. Therefore, in the following we will always assume that $|\hat{t}| \leq |\hat{u}|$ and that

$$\hat{t} = -\frac{1}{2}\left(\hat{s} - m_3^2 - m_4^2 - \sqrt{\lambda(\hat{s}, m_3^2, m_4^2) - 4\hat{s}\, p_T^2}\right), \tag{2.3}$$

where $\lambda(a, b, c) = a^2 + b^2 + c^2 - 2ab - 2ac - 2bc$ is the Källén function.

In the forward regime, the validity of both the p_T and HE expansions is limited by the condition

$$|\hat{t}| \simeq 4m_t^2, \tag{2.4}$$

i.e. for any fixed value of $\hat{s}$, the p_T expansion provides reliable results when $|\hat{t}| \lesssim 4m_t^2$ while the HE expansion is accurate for $|\hat{t}| \gtrsim 4m_t^2$, if the fixed $\hat{s} > 4m_t^2$. However, we find that in the vicinity of the point $|\hat{t}| = 4m_t^2$ the fixed-order results in the p_T expansion and in the HE expansion are both divergent (see figure 1). As a consequence, a straightforward combination of the p_T-expanded and the HE-expanded results cannot allow for an accurate description of the above region, and this fact prevents a full coverage of the phase space. We point out that this situation does not change substantially when higher orders in both the expansions are computed.

Alternatively, the convergence of the expanded results can be improved by considering the respective Padé approximants. Indeed, starting from a given Taylor expansion of an exact function $f(x)$ around $x = 0$ up to the first r terms

$$f(x) \simeq \sum_{k=0}^{r-1} c_k x^k, \tag{2.5}$$

it is possible to construct the associated Padé approximant, defined as

$$[m/n](x) = \frac{p_0 + p_1 x + \cdots + p_m x^m}{1 + q_1 x + \ldots q_n x^n}, \tag{2.6}$$

provided that $m + n + 1 = r$. Specifically, by Taylor-expanding the r.h.s. of eq. (2.6), the $\{p_i, q_j\}$ coefficients of the Padé approximant can be written in terms of the c_k ones known from eq. (2.5), by solving a system of linear equations. Usually, $[m/n]$ Padé approximants such that $m = n$ give the best improvement in the convergence of the original Taylor expansion, and we consider only these combinations in our study. In the p_T-expanded results, at NLO, only the first three terms in eq. (2.5) are known and therefore we are limited to construct a [1/1] Padé approximant (we will refer to this as the p_T-Padé). Instead the availability of many terms in the HE-expansion results allows to consider several $[n/n]$ approximants (defined as HE-Padé).

When calculating the p_T-Padé, care is to be taken in the treatment of the expansion parameters. As discussed in refs. [18, 19], not only the p_T but also the masses of the external particles are understood as small parameters. Since these are all treated on the same footing

JHEP07(2022)069

with respect to the large scales set by $\hat{s}$ and m_t, we can write the general expression for a p_T-expanded form factor F in the amplitude in terms of a scaling parameter x

$$F(x) = \sum_{N=0}^{2} x^N \sum_{i+j+k=N} c_{ijk}\ (p_T^2)^i (m_3^2)^j (\Delta_m)^k \equiv \sum_{N=0}^{2} x^N c_N \tag{2.7}$$

where m_3 is interpreted as m_H and m_Z for $gg \to HH$ and $gg \to ZH$, respectively, and $\Delta_m = (m_4^2 - m_3^2)/2$ is included only for the ZH case (see ref. [19]). Starting from eq. (2.7) we can then obtain the corresponding [1/1] Padé approximant with respect to the limit $x \to 0$

$$[1/1](x) = \frac{p_0 + p_1 x}{1 + q_1 x}, \tag{2.8}$$

with

$$p_0 = c_0 \qquad p_1 = c_1 - \frac{c_0 c_2}{c_1} \qquad q_1 = -\frac{c_2}{c_1},$$

and subsequently set $x = 1$ in eq. (2.8).

We want to clarify a possible source of ambiguity concerning the limit of validity of the p_T expansion. Indeed, while in the previous works we suggested that this expansion is valid for $p_T^2 \lesssim 4m_t^2$, as the comparison at LO between the p_T-expanded and exact result seems to indicate, in this paper we follow a more conservative approach and we consider as limit of validity for the p_T expansion $|\hat{t}| \lesssim 4m_t^2$. Additionally, we checked that the same complementarity for the p_T and HE expansions can be observed when choosing $p_T^2 = 4m_t^2$ as limit of validity.

We now discuss the procedure adopted to construct the Padé approximants from the HE expansion. Following the prescription of ref. [29] (see also [30, 31]), we initially arrange the various orders $F^{(i)}$ of the HE expansion for a given form factor as follows

$$F(x) = F^{(0)} + \sum_{l=1}^{L} \left(F^{(2l-1)} m_t^{(2l-1)} + F^{(2l)} m_t^{(2l)} \right) x^l = \sum_{l=0}^{L} d_l x^l, \tag{2.9}$$

where orders related to odd powers of m_t are grouped with the orders related to the next even power. Then, we construct $[n/n]$ approximants in x with $2n = L$ from eq. (2.9) using the analytic expressions available in [32, 33], and setting $x = 1$. We remark that our Padé approximants are obtained in a fully symbolic way, whereas in refs. [29, 30] all the kinematical quantities are fixed to the respective numerical values before the Padés are constructed in x. Furthermore, in comparison to refs. [23, 29], we only studied $[n/n]$ HE-Padés up to $n = 6$. In those references Padés with $n > 6$ were also considered in order to extrapolate the results in the region $|\hat{t}| < 4m_t^2$, for a fixed $\hat{s}$, and characterize the relative uncertainties of different $[m/n]$ Padés. In our case, because the region $|\hat{t}| < 4m_t^2$, is more accurately described by the results of the p_T expansion, we find that a [6/6] HE-Padé is more than enough to perform the merging with the p_T-result and, at the same time, to describe accurately the high-energy region.

The p_T-Padé and the HE-Padé extend the range of validity of each expansion beyond its limit. As discussed in the next section, the p_T and the HE Padés are accurate enough to bridge the gap around the phase-space region $|\hat{t}| \simeq 4m_t^2$. Then, an accurate approximation

JHEP07(2022)069

of the exact result for any phase-space point $(\hat{s}, \hat{t})$ can be obtained by choosing as switching point between the Padé-improved expansions any point in the region $|\hat{t}| \sim 4m_t^2$. For simplicity we choose to use the p_T-Padé when $|\hat{t}| < 4m_t^2$ and the HE-Padé when $|\hat{t}| \geq 4m_t^2$, for any fixed value of $\hat{s}$. We recall that in our discussion we just consider the forward region $|\hat{t}| \leq |\hat{u}|$, while the result in the complementary phase-space region is obtained using the symmetry of our form factors under $\hat{t} \leftrightarrow \hat{u}$. Noticing that, when $|\hat{t}| \leq |\hat{u}|$, the maximum absolute value of $\hat{t}$ as a function of $\hat{s}$ is given by $|\hat{t}|_{\max} = 1/2(\hat{s} - m_3^2 - m_4^2)$ our choice corresponds to using the p_T-Padé up to the partonic energy $\hat{s}_c = 8m_t^2 + m_3^2 + m_4^2$. In this energy region ($\sqrt{\hat{s}_c} \simeq 500\,\text{GeV}$ for $gg \to HH$ and $gg \to ZH$) at the LHC more than 2/3 of the hadronic cross section is concentrated.

3 The p_T and HE expansions vs the exact results at LO

In this section we assess the reliability of our merging procedure by studying how well the combination of the p_T-Padé and the HE-Padé can reproduce the exact LO results for HH and ZH production via gluon fusion. For the sake of simplicity, we discuss in detail only the $gg \to HH$ process, but we verified that similar conclusions can be drawn for $gg \to ZH$.

Using the same notation of ref. [16], we recall that the amplitude for $gg \to HH$ can be expressed as

$$A^{\mu\nu} = \frac{G_\mu}{\sqrt{2}} \frac{\alpha_S(\mu_R)}{2\pi} \delta_{ab} T_F \hat{s} [A_1^{\mu\nu} F_1 + A_2^{\mu\nu} F_2], \tag{3.1}$$

where F_1 and F_2 are the form factors associated to the spin-0 and spin-2 projectors, respectively. Both triangle and box diagrams contribute to F_1

$$F_1 = F_\triangle \frac{3m_H^2}{\hat{s} - m_H^2} + F_\square, \tag{3.2}$$

whereas the F_2 form factor receives contribution only from boxes. Our goal is to improve the evaluation of the box contributions, therefore we focus on the discussion of $F_\square$ and F_2.

The LO results for these form factors, denoted as $F_\square^{\text{LO}}$ and F_2^{LO}, are shown in figure 1, for fixed values of the partonic center-of-mass energy. Only large values of $\hat{s}$ are shown in figure 1 because for small $\hat{s}$ values the p_T-expanded results are very accurate [18]. The p_T-expanded and HE-expanded results are represented by the blue and purple solid lines, respectively, and they deviate from the exact result, shown as a solid black line, at $|\hat{t}|/4m_t^2 \simeq 1$, as anticipated in the previous section. The light blue dashed line stands for the [1/1] p_T-Padé, while the pink dashed line represents the [6/6] HE-Padé. One can see that the Padé results show an improved convergence with respect to the fixed-order expansions. The bottom part of the plots in figure 1 shows the ratio of the expanded and Padé results to the exact one. Indeed, figure 1(a,b) shows that in the case of $F_\square^{\text{LO}}$ for $|\hat{t}|/4m_t^2 = 1$ the differences of the Padé results with respect to the exact prediction are negligible. For the F_2 form factor, whose contribution to the cross-section is much smaller than the one of the F_1 form factor, the difference is always below 5%, see figure 1(c,d). We notice that, when comparing the accuracies of the Padé approximants, larger discrepancies can be attributed to the p_T-Padé. Indeed, being the latter a [1/1] Padé, it is expected to be a less refined approximation

JHEP07(2022)069

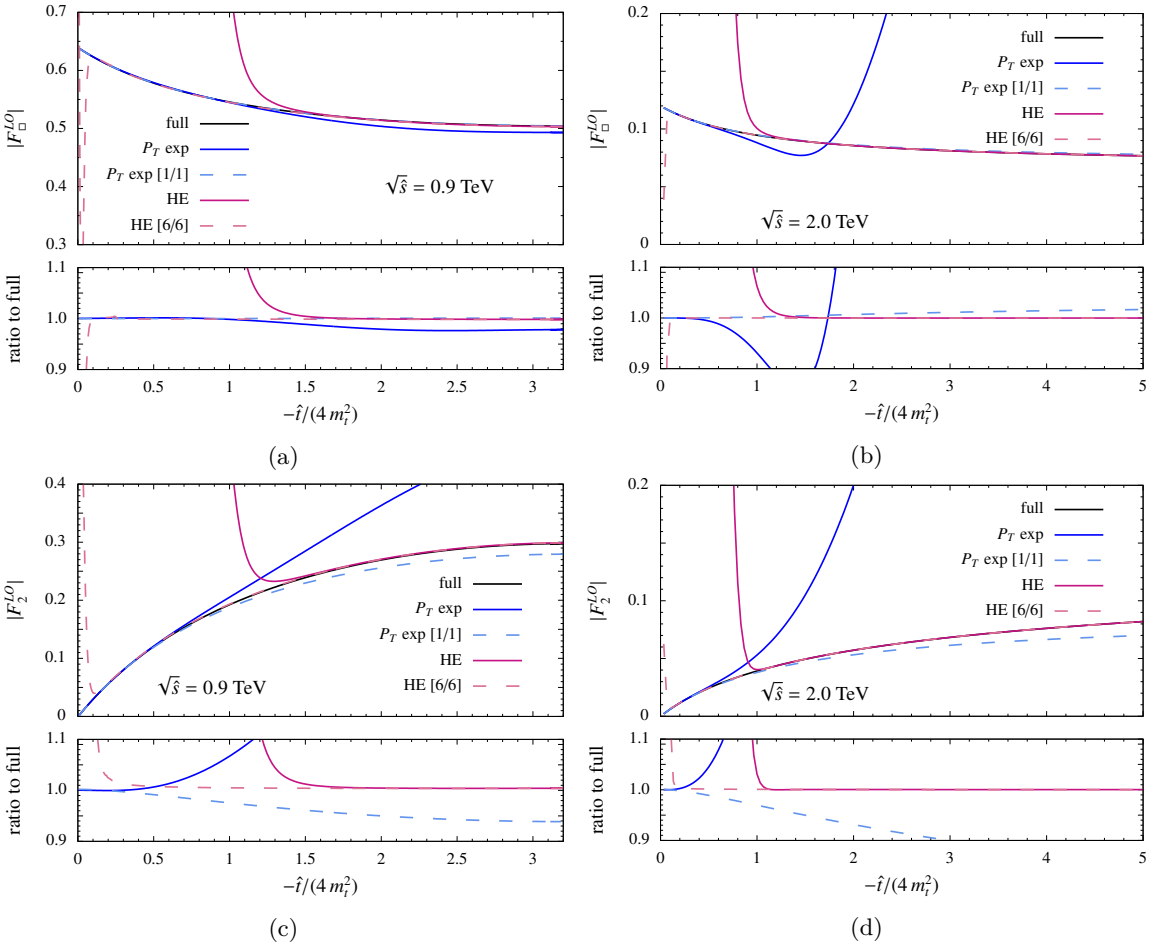

Figure 1. Modulus of the box form factors contributing to $gg \to HH$ at LO, for a fixed value of (a,c) $\sqrt{\hat{s}} = 0.9\,\text{TeV}$ and (b,d) $\sqrt{\hat{s}} = 2\,\text{TeV}$. In the upper part of each plot, the exact prediction (solid black line) is shown together with the p_T and HE expansions (solid blue and purple lines, respectively) and with the [1/1] p_T and [6/6] HE Padé approximants (dashed light blue and pink lines, respectively). The bottom part of each plot shows the ratio of the above results to the exact prediction.

than the [6/6] HE-Padé. Still, in the case of $F_\square^{\text{LO}}$ the differences between the two Padé near $|\hat{t}|/4m_t^2 = 1$ are negligible. We also notice that, as $\hat{s}$ increases, larger values of $|\hat{t}|$ are allowed by the kinematics, and the relative importance of the HE expansion increases.

The improvement in convergence provided by the Padé approximants is such that the merging of the two results discussed in the previous section can reproduce the exact prediction with good accuracy for every value of $\hat{t}$, for any $\hat{s}$. While we refrain from showing more examples here, we note that we studied the behaviour of all the box contributions to $gg \to HH$ and $gg \to ZH$ at several values of $\hat{s}$. We explicitly checked that, among the various possibilities, a [6/6] HE-Padé is more than enough for an accurate merging. Furthermore, we observed that the value $|\hat{t}| = 4m_t^2$ is a good choice as a merging point for the p_T and HE Padé approximants. The high level of accuracy of our merging method can be observed in figure 2, where the partonic cross section at LO is shown for $gg \to HH$ and

JHEP07(2022)069

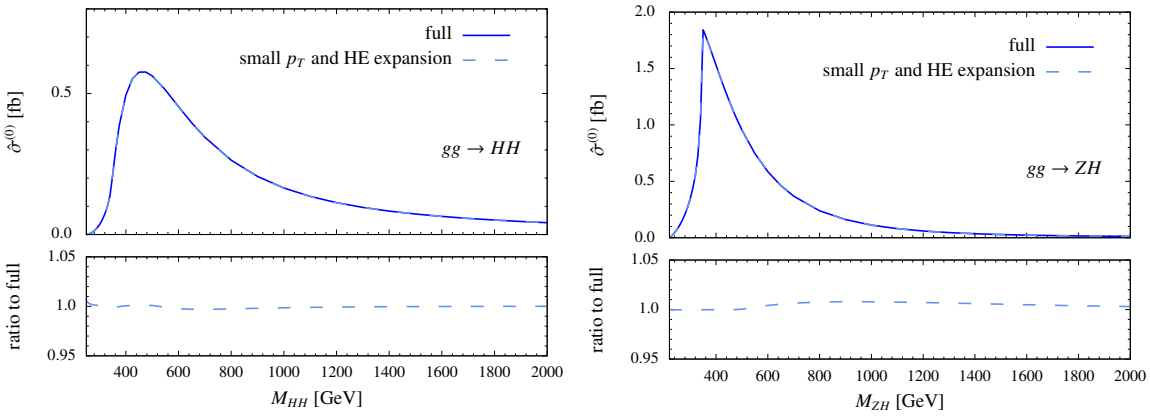

(a) (b)

Figure 2. Partonic cross section at LO for (a) $gg \to HH$ and (b) $gg \to ZH$. The upper part of each plot shows the exact prediction (solid line) together with the merging of the p_T and HE Padé approximants (dashed line). The bottom part of each plot shows the ratio of the merged result to the exact prediction.

$gg \to ZH$. One can see that deviations of the combination of the p_T- and HE-Padé with respect to the exact prediction never exceed 1%.

4 Merging the p_T and HE expansions at NLO

In the previous section we showed that the merging of the p_T- and HE-Padé can accurately reproduce the exact LO prediction. In this section we present the merging of the NLO p_T-expanded and HE-expanded results improved by the respective Padé approximants.

In figure 3 the NLO contributions to $F_\square$ and F_2 are shown.[3] The relative behaviour of the various approximations is analogous to what we observed at LO. For low values of $|\hat{t}|$ the fixed-order and Padé-improved p_T-expanded results agree well. Increasing the value of $|\hat{t}|$ up to the merging region, $|\hat{t}| \sim 4m_t^2$, the p_T-Padé becomes close to the Padé-improved HE expansion. For values above $|\hat{t}| = 4m_t^2$ the p_T and HE Padé approximants show small deviations as expected. The NLO study shows the same qualitative behaviour as the LO one. This makes us confident that the proposed merging procedure works well also at NLO.

We now compare our evaluation of the virtual corrections for the di-Higgs production process[4] with the numerical result provided as a grid in ref. [34]. This reference summarizes the work of ref. [29], where the numerical calculation in exact top-mass dependence of ref. [8] was supplemented by the result in the HE expansion of ref. [22]. The comparison is done on the quantity

$$\Delta\hat{\sigma}_{\text{virt}} = \int_{\hat{t}_-}^{\hat{t}_+} \frac{\alpha_s}{32\pi^2}\frac{1}{\hat{s}^2}\mathcal{V}_{\text{fin}}d\hat{t}, \tag{4.1}$$

[3] $F_\square^{\text{NLO}}$ and F_2^{NLO} are the form factors as defined in eq. (3.1) but do not contain the double triangle diagrams that can be expressed in terms of products of one-loop integrals and as such are computed analytically in exact top-mass dependence [16].

[4] We note that for ZH production no public code including the results of the full computation [11] is currently available. Hence we refrain from making any comparisons for ZH production.

JHEP07(2022)069

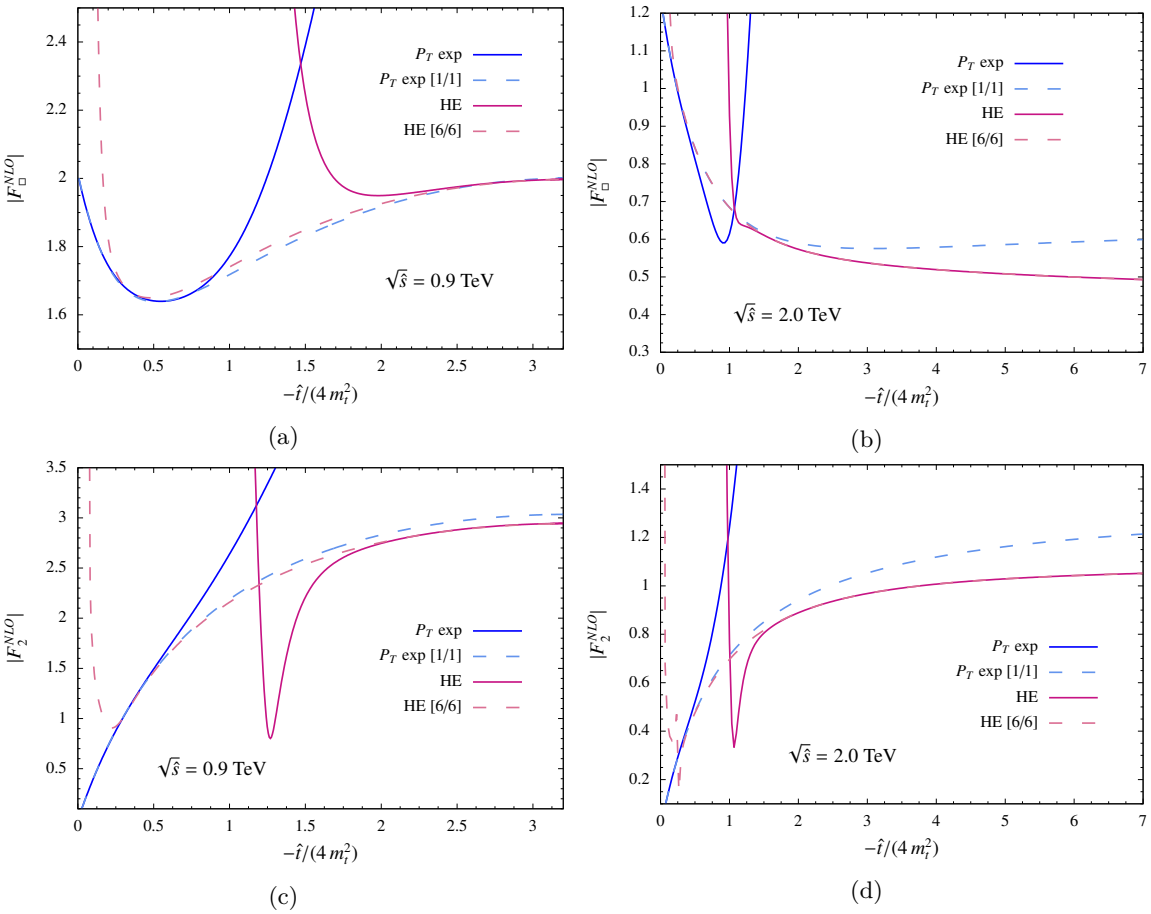

Figure 3. Modulus of the box form factors contributing to $gg \to HH$ at NLO, for a fixed value of (a,c) $\sqrt{\hat{s}} = 0.9\,\text{TeV}$ and (b,d) $\sqrt{\hat{s}} = 2\,\text{TeV}$. The p_T and HE expansions are shown as solid blue and purple lines, respectively, while the [1,1] p_T- and [6,6] HE-Padé are shown as dashed light blue and pink lines, respectively.

where the finite part of the virtual corrections $\mathcal{V}_{\text{fin}}$ is defined as in ref. [27]. The results are shown in figure 4. We note that $\mathcal{V}_{\text{fin}}$ depends on the choice of the IR subtraction, this is why in the lower panel of figure 4 the difference between the expanded results and the numerical grid of ref. [29] is shown (divided by the Born result), a quantity that is independent of the IR subtraction term. The grid of ref. [34] shows very good agreement with our results at every invariant mass, except for the first few bins at low M_{HH}. The reason is a large uncertainty of the numerical grid on the low M_{HH} bins, that are described by only a few points in the numerical grid due to their small contribution to the total cross section. For moderate and large M_{HH} we observe differences below 1% in the ratio between our results and the ones of ref. [29]. We confirm these findings by comparing our results for $\mathcal{V}_{\text{fin}}$ with the values given in the grid [34] for various points at fixed $(M_{HH}, \hat{t})$. We find a good agreement, as can be inferred from table 1 for some representative values. We notice that in the region where both expansions perform less well we see differences of a few percent, although the latter will be reduced in $\Delta\hat{\sigma}_{\text{virt}}$ due to the integration over $\hat{t}$.

JHEP07(2022)069

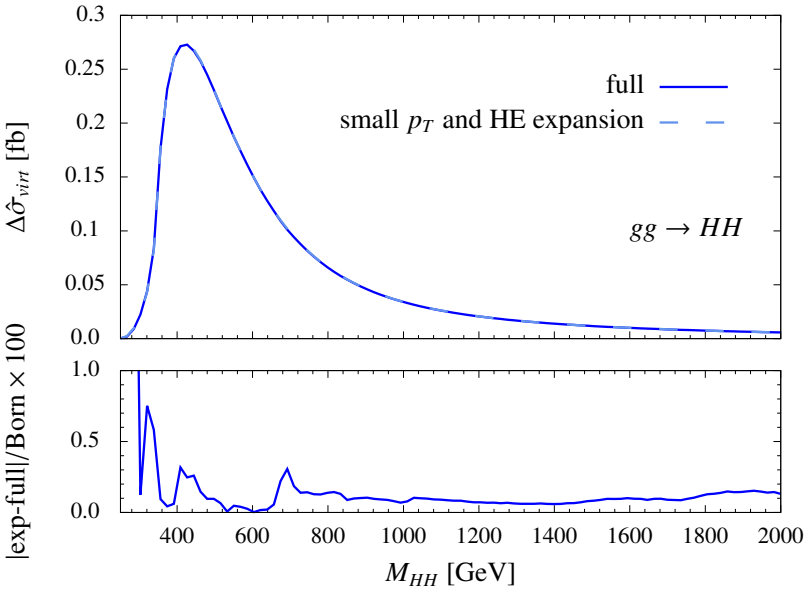

Figure 4. Upper panel: $\Delta\hat{\sigma}_{\text{virt}}$ using the numerical grid provided in ref. [29] (dark blue line) and our combination of HE expansion and small p_T expansion (light blue dashed line). The lower panel shows the absolute value of the difference between the two results, normalized to the partonic LO cross section.

M_{HH} [GeV]	$\hat{t}$ [GeV^2]	$\mathcal{V}_{\text{fin}}^{\text{Pade}}$	$\mathcal{V}_{\text{fin}}^{\text{grid}}$
280.9	$-7.783 \cdot 10^3$	$9.548 \cdot 10^{-6}$	$9.410 \cdot 10^{-6}$
411.4	$-6.627 \cdot 10^4$	$4.520 \cdot 10^{-4}$	$4.510 \cdot 10^{-4}$
586.96	$-6.925 \cdot 10^4$	$4.930 \cdot 10^{-4}$	$4.943 \cdot 10^{-4}$
716.55	$-1.816 \cdot 10^5$	$4.430 \cdot 10^{-4}$	$4.298 \cdot 10^{-4}$
1048.93	$-2.133 \cdot 10^5$	$2.952 \cdot 10^{-4}$	$3.104 \cdot 10^{-4}$
1855.32	$-1.678 \cdot 10^6$	$2.497 \cdot 10^{-4}$	$2.498 \cdot 10^{-4}$

Table 1. Comparison of various numerical values of $\mathcal{V}_{\text{fin}}$ taken from the grid of ref. [34] with our Padé construction.

Finally, we show that our merging approach is flexible with respect to the modification of the input parameters by computing the virtual corrections for various renormalisation schemes of the top quark mass. It was noted in refs. [9, 10] that the di-Higgs production process suffers from a large uncertainty associated to the renormalisation scheme of the top quark mass. In particular, an uncertainty on the NLO cross section between +4% and −18% [35] is related to the change from the on-shell renormalisation scheme to the $\overline{\text{MS}}$ scheme for the top mass, with the latter evaluated at different values of the renormalisation scale (m_t, M_{HH} and $M_{HH}/4$). The results presented so far have been calculated using the on-shell scheme for the top mass, however the form factors in the $\overline{\text{MS}}$ scheme can be

JHEP07(2022)069

obtained by simply shifting our result according to:

$$F_i^{\text{NLO},\overline{\text{MS}}} = F_i^{\text{NLO,OS}} - \frac{1}{4}\frac{\partial F_i^{\text{LO}}}{\partial m_t^2}\Delta_{m_t^2} \tag{4.2}$$

with $i = \Delta, \square, 2$ and

$$\Delta_{m_t^2} = 2m_t^2 C_F \left[-4 + 3\log\left(\frac{m_t^2}{\mu^2}\right)\right] . \tag{4.3}$$

Notice that the numerical values for the top quark mass have to be adjusted to their $\overline{\text{MS}}$ values, which we evaluate following refs. [36, 37]. Since the LO results are available analytically, we can first build the Padé approximants of the p_T- or HE-expanded $F_i^{\text{NLO,OS}}$ form factors and then calculate the shift to the $\overline{\text{MS}}$ scheme using the full LO form factors in eq. (4.2). Alternatively, we can use the expanded LO form factors to perform the shift in eq. (4.2) order by order in the p_T-expanded and the HE-expanded results, and then build Padé approximants on the $F_i^{\text{NLO},\overline{\text{MS}}}$ form factors. The difference between these two approaches turns out to be well below the 0.5 permille level everywhere except near the top-mass threshold where the difference is at the percent level. For the $gg \to ZH$ process, the shift to the $\overline{\text{MS}}$ scheme can be applied in analogy to eq. (4.2) on the associated form factors.[5] For the triangle contributions we always use the results available in full top-mass dependence.

We present our results in figure 5. We observe that indeed the $\Delta\hat{\sigma}_{\text{virt}}$ show a non-negligible dependence on the renormalisation scheme for the top quark mass. This holds true both for $gg \to HH$ and for $gg \to ZH$. In particular, for $gg \to ZH$ we see a shift of the maximal value of the differential $\Delta\hat{\sigma}_{\text{virt}}$, which is associated to the lower top quark mass value. This may point to a significant uncertainty related to the top-mass scheme also in the case of $gg \to ZH$. We notice, however, that the effects observed in figure 5 are likely to be partially compensated by similar modifications in the LO cross section and by the inclusion of the real-emission corrections at NLO. Therefore, we use figure 5 only as an illustration of the flexibility of the merging method discussed in this paper, and we leave a full assessment of the effects due the change of the top-mass renormalisation scheme to a future work. For the same reason we refrain from providing a full comparison with ref. [35] for $gg \to HH$.

5 Conclusion

In this paper, we combined an expansion in small p_T with a HE expansion for the processes $gg \to HH$ and $gg \to ZH$ and we showed that this combination leads to results that describe the whole phase space of the considered processes with high accuracy.

The expansion in small p_T is valid for $|\hat{t}| \lesssim 4m_t^2$, while the HE expansion is valid for $|\hat{t}| \gtrsim 4m_t^2$ and $\hat{s} > 4m_t^2$. For a successful combination of the two expansion methods, we extended the validity range of both expansions making use of simple Padé approximants. This allowed us to describe also the region $|\hat{t}| \simeq 4m_t^2$ very accurately.

We verified our method first at LO, where exact analytic results are available. At the level of the differential partonic cross section, the difference with the results in exact top

[5] The $\Delta\hat{\sigma}_{\text{virt}}$ for $gg \to ZH$ was defined as in ref. [19].

JHEP07(2022)069

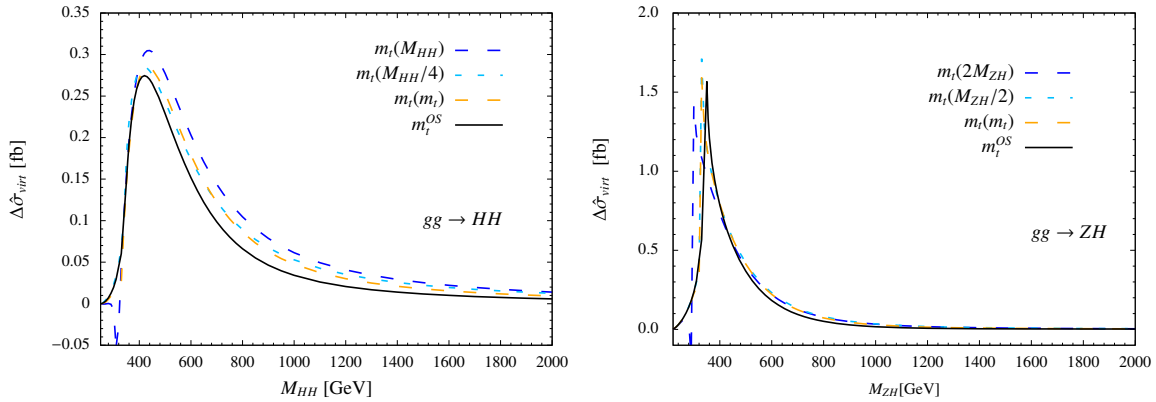

(a) (b)

Figure 5. The integrated virtual corrections in different renormalisation schemes for the top quark mass for (a) $gg \to HH$ and (b) $gg \to ZH$. The dashed lines show $\Delta\hat{\sigma}_{\rm virt}$ in the $\overline{\rm MS}$ scheme using the top quark mass evaluated at different choices of the renormalisation scale, while the black solid line shows the on-shell result.

quark mass dependence never exceeded 1% for any of the M_{HH} bins. In a second step, we compared our results with a numerical grid containing the results of a computation in exact top quark mass dependence for the $gg \to HH$ process [29]. Also at NLO we could verify the good numerical accuracy of our approach, observing differences below 1% for the invariant mass bins where the numerical accuracy of the grid is assumed to be sufficiently high.

We have also shown that in our analytic calculation the top quark mass renormalisation scheme can be easily changed. This shows the great flexibility of our analytic approach with respect to the numerical one. With a running time of well below 1 s per phase-space point our results can be well implemented in a fast and versatile Monte Carlo program.

Acknowledgments

We thank Lina Alasfar and Xiaoran Zhao for useful discussions. We would also like to thank the authors of ref. [23] for a careful reading of the manuscript and for their useful comments. G.D. would like to thank the Department of Physics of the University of Rome "La Sapienza" for the kind hospitality during part of this project. The work of G.D. and M.V. was partially supported by the Italian Ministry of Research (MUR) under grant PRIN 20172LNEEZ. The work of L.B. and P.P.G. has received financial support from Xunta de Galicia (Centro singular de investigación de Galicia accreditation 2019-2022), by European Union ERDF, and by "María de Maeztu" Units of Excellence program MDM-2016-0692 and the Spanish Research State Agency.

Open Access. This article is distributed under the terms of the Creative Commons Attribution License (CC-BY 4.0), which permits any use, distribution and reproduction in any medium, provided the original author(s) and source are credited. SCOAP^3 supports the goals of the International Year of Basic Sciences for Sustainable Development.

JHEP07(2022)069

References

[1] S. Catani, D. de Florian, M. Grazzini and P. Nason, *Soft gluon resummation for Higgs boson production at hadron colliders*, *JHEP* **07** (2003) 028 [hep-ph/0306211] [INSPIRE].

[2] V. Ahrens, T. Becher, M. Neubert and L.L. Yang, *Origin of the large perturbative corrections to Higgs production at hadron colliders*, *Phys. Rev. D* **79** (2009) 033013 [arXiv:0808.3008] [INSPIRE].

[3] M. Spira, A. Djouadi, D. Graudenz and P.M. Zerwas, *Higgs boson production at the LHC*, *Nucl. Phys. B* **453** (1995) 17 [hep-ph/9504378] [INSPIRE].

[4] R. Harlander and P. Kant, *Higgs production and decay: analytic results at next-to-leading order QCD*, *JHEP* **12** (2005) 015 [hep-ph/0509189] [INSPIRE].

[5] U. Aglietti, R. Bonciani, G. Degrassi and A. Vicini, *Analytic results for virtual QCD corrections to Higgs production and decay*, *JHEP* **01** (2007) 021 [hep-ph/0611266] [INSPIRE].

[6] C. Anastasiou, S. Beerli, S. Bucherer, A. Daleo and Z. Kunszt, *Two-loop amplitudes and master integrals for the production of a Higgs boson via a massive quark and a scalar-quark loop*, *JHEP* **01** (2007) 082 [hep-ph/0611236] [INSPIRE].

[7] S. Borowka, G. Heinrich, S.P. Jones, M. Kerner, J. Schlenk and T. Zirke, *SecDec-3.0: numerical evaluation of multi-scale integrals beyond one loop*, *Comput. Phys. Commun.* **196** (2015) 470 [arXiv:1502.06595] [INSPIRE].

[8] S. Borowka et al., *Higgs boson pair production in gluon fusion at next-to-leading order with full top-quark mass dependence*, *Phys. Rev. Lett.* **117** (2016) 012001 [*Erratum ibid.* **117** (2016) 079901] [arXiv:1604.06447] [INSPIRE].

[9] J. Baglio, F. Campanario, S. Glaus, M. Mühlleitner, M. Spira and J. Streicher, *Gluon fusion into Higgs pairs at NLO QCD and the top mass scheme*, *Eur. Phys. J. C* **79** (2019) 459 [arXiv:1811.05692] [INSPIRE].

[10] J. Baglio et al., *Higgs-pair production via gluon fusion at hadron colliders: NLO QCD corrections*, *JHEP* **04** (2020) 181 [arXiv:2003.03227] [INSPIRE].

[11] L. Chen, G. Heinrich, S.P. Jones, M. Kerner, J. Klappert and J. Schlenk, *ZH production in gluon fusion: two-loop amplitudes with full top quark mass dependence*, *JHEP* **03** (2021) 125 [arXiv:2011.12325] [INSPIRE].

[12] S. Dawson, S. Dittmaier and M. Spira, *Neutral Higgs boson pair production at hadron colliders: QCD corrections*, *Phys. Rev. D* **58** (1998) 115012 [hep-ph/9805244] [INSPIRE].

[13] L. Altenkamp, S. Dittmaier, R.V. Harlander, H. Rzehak and T.J.E. Zirke, *Gluon-induced Higgs-strahlung at next-to-leading order QCD*, *JHEP* **02** (2013) 078 [arXiv:1211.5015] [INSPIRE].

[14] J. Grigo, J. Hoff, K. Melnikov and M. Steinhauser, *On the Higgs boson pair production at the LHC*, *Nucl. Phys. B* **875** (2013) 1 [arXiv:1305.7340] [INSPIRE].

[15] J. Grigo, J. Hoff and M. Steinhauser, *Higgs boson pair production: top quark mass effects at NLO and NNLO*, *Nucl. Phys. B* **900** (2015) 412 [arXiv:1508.00909] [INSPIRE].

[16] G. Degrassi, P.P. Giardino and R. Gröber, *On the two-loop virtual QCD corrections to Higgs boson pair production in the Standard Model*, *Eur. Phys. J. C* **76** (2016) 411 [arXiv:1603.00385] [INSPIRE].

JHEP07(2022)069

[17] A. Hasselhuhn, T. Luthe and M. Steinhauser, *On top quark mass effects to $gg \to ZH$ at NLO*, *JHEP* **01** (2017) 073 [arXiv:1611.05881] [INSPIRE].

[18] R. Bonciani, G. Degrassi, P.P. Giardino and R. Gröber, *Analytical method for next-to-leading-order QCD corrections to double-Higgs production*, *Phys. Rev. Lett.* **121** (2018) 162003 [arXiv:1806.11564] [INSPIRE].

[19] L. Alasfar, G. Degrassi, P.P. Giardino, R. Gröber and M. Vitti, *Virtual corrections to $gg \to ZH$ via a transverse momentum expansion*, *JHEP* **05** (2021) 168 [arXiv:2103.06225] [INSPIRE].

[20] R. Bonciani, G. Degrassi, P.P. Giardino and R. Gröber, *A numerical routine for the crossed vertex diagram with a massive-particle loop*, *Comput. Phys. Commun.* **241** (2019) 122 [arXiv:1812.02698] [INSPIRE].

[21] J. Davies, G. Mishima, M. Steinhauser and D. Wellmann, *Double-Higgs boson production in the high-energy limit: planar master integrals*, *JHEP* **03** (2018) 048 [arXiv:1801.09696] [INSPIRE].

[22] J. Davies, G. Mishima, M. Steinhauser and D. Wellmann, *Double Higgs boson production at NLO in the high-energy limit: complete analytic results*, *JHEP* **01** (2019) 176 [arXiv:1811.05489] [INSPIRE].

[23] J. Davies, G. Mishima and M. Steinhauser, *Virtual corrections to $gg \to ZH$ in the high-energy and large-m_t limits*, *JHEP* **03** (2021) 034 [arXiv:2011.12314] [INSPIRE].

[24] X. Xu and L.L. Yang, *Towards a new approximation for pair-production and associated-production of the Higgs boson*, *JHEP* **01** (2019) 211 [arXiv:1810.12002] [INSPIRE].

[25] G. Wang, Y. Wang, X. Xu, Y. Xu and L.L. Yang, *Efficient computation of two-loop amplitudes for Higgs boson pair production*, *Phys. Rev. D* **104** (2021) L051901 [arXiv:2010.15649] [INSPIRE].

[26] G. Wang, X. Xu, Y. Xu and L.L. Yang, *Next-to-leading order corrections for $gg \to ZH$ with top quark mass dependence*, *Phys. Lett. B* **829** (2022) 137087 [arXiv:2107.08206] [INSPIRE].

[27] R. Gröber, A. Maier and T. Rauh, *Reconstruction of top-quark mass effects in Higgs pair production and other gluon-fusion processes*, *JHEP* **03** (2018) 020 [arXiv:1709.07799] [INSPIRE].

[28] J. Davies, R. Gröber, A. Maier, T. Rauh and M. Steinhauser, *Padé approach to top-quark mass effects in gluon fusion amplitudes*, *PoS* **RADCOR2019** (2019) 079 [arXiv:1912.04097] [INSPIRE].

[29] J. Davies et al., *Double Higgs boson production at NLO: combining the exact numerical result and high-energy expansion*, *JHEP* **11** (2019) 024 [arXiv:1907.06408] [INSPIRE].

[30] J. Davies, G. Mishima, M. Steinhauser and D. Wellmann, *$gg \to ZZ$: analytic two-loop results for the low- and high-energy regions*, *JHEP* **04** (2020) 024 [arXiv:2002.05558] [INSPIRE].

[31] D. Wellmann, *Top quark mass effects in Higgs and Z boson pair production and Higgs boson decays*, Ph.D. thesis, KIT, Karlsruhe, Germany (2020).

[32] *TTP*19-018 *Double Higgs boson production at NLO: combining the exact numerical result and high-energy expansion*, https://www.ttp.kit.edu/preprints/2019/ttp19-018/.

JHEP07(2022)069

[33] *TTP*20-041 *Virtual corrections to $gg \to ZH$ in the high-energy and large-m_t limits*, https://www.ttp.kit.edu/preprints/2020/ttp20-041/.

[34] *hhgrid GitHub page*, https://github.com/mppmu/hhgrid.

[35] J. Baglio, F. Campanario, S. Glaus, M. Mühlleitner, J. Ronca and M. Spira, *$gg \to HH$: combined uncertainties*, *Phys. Rev. D* **103** (2021) 056002 [arXiv:2008.11626] [INSPIRE].

[36] K. Melnikov and T.v. Ritbergen, *The three loop relation between the MS-bar and the pole quark masses*, *Phys. Lett. B* **482** (2000) 99 [hep-ph/9912391] [INSPIRE].

[37] M. Carena, D. Garcia, U. Nierste and C.E.M. Wagner, *Effective Lagrangian for the $\bar{t}bH^+$ interaction in the MSSM and charged Higgs phenomenology*, *Nucl. Phys. B* **577** (2000) 88 [hep-ph/9912516] [INSPIRE].

JHEP07(2022)069